ACCEPTED MANUSCRIPT

Spectral characterization and antimicrobial activity studies of 5,6-dichloro-1*H*-benzimidazol-2-yl-(4'/5'/6'-substituted)-phenols (HL₁ – HL₂₀) and Co(II), Ni(II), Cu(II), Zn(II) and Pd(II) complexes of HL₁

AYDIN TAVMAN[1]*, DEMET GURBUZ[2], MAYRAM HACIOGLU[3], ADEM CINARLI[2], ONUR SAHIN[4] AND A. SEHER BIRTEKSOZ TAN[3]

[1]Istanbul University-Cerrahpaşa, Faculty of Engineering, Department of Chemistry, Inorganic Chemistry Division, 34320 Avcilar, Istanbul, Türkiye, [2]Istanbul University-Cerrahpaşa, Faculty of Engineering, Department of Chemistry, Organic Chemistry Division, 34320 Avcilar, Istanbul, Türkiye, [3]Istanbul University, Faculty of Pharmacy, Department of Pharmaceutical Microbiology, 34452 Beyazit, Istanbul, Türkiye, and [4]Sinop University, Faculty of Health Sciences, Department of Occupational Health and Safety, 57000 Sinop, Türkiye.

Abstract: 5,6-Dichloro-1*H*-benzimidazol-2-yl-(4'/5'/6'-substituted)-phenols (**HL₁ – HL₂₀**) and MCl₂ complexes (M: Co, Ni, Cu, Zn, Pd) of **HL₁** were synthesized and characterized by various physico-chemical and spectroscopic methods such as elemental analysis, thermogravimetric analysis, FTIR, NMR and fluorescence spectroscopy. The structures of the complexes were also confirmed by performing molar conductivity and magnetic moment measurements. **HL₁** acted as a bidentate, monobasic chelating ligand with NO donor sites in all the complexes. It was found that all complexes have non-electrolytic properties and the M:L ratios are 1:1 in the Zn(II) complex and 1:2 in the other complexes. Crystal structure of **HL₁₈** was also investigated. The presence of both intra- and inter-molecular hydrogen bonding was observed in both molecules. According to the fluorescence spectral data, the substituents at the 4-position made the fluorescence emission shifted to the lower wavelengths (redshift) compared to **HL₁**, while the substituents at the 3- and 5-positions caused a blueshift effect. The Zn(II) complex showed a greater redshift effect compared to the other complexes. In addition, antimicrobial activity of the compounds was evaluated against six bacteria and three fungi. It was observed that **HL₁** and its mono substituted derivatives (**HL₁ – HL₁₁**) show selective activity especially against Gram positive bacteria, *S. aureus* and *S. epidermidis*. Zn(II) complex showed relatively higher activity against Gram positive bacteria differently from the other complexes.

INTRODUCTION

It is known that many benzimidazole derivatives play a role in the field of pharmacology as the active ingredient of many drugs. For example, 4-{5-[bis(2-chloroethyl)amino]-1-methyl-2-bezimidazolyl}butyric acid hydrochloride, also known as Bendamustine and used as a chemotherapy agent, is one of them.[1,2] Perhaps the well-known one is Omeprazole, [5-methoxy-2-(4-methoxy-3,5-dimethylpyridin-2-yl-methylsulphinyl)-1*H*-benzimidazole], an antisecretory agent.[3] Other important benzimidazole derivatives used as drugs include thiabendazole,[4,5] albendazole, mebendazole, flubendazole,[6,7] astemizole[8] and fenbendazole.[9]
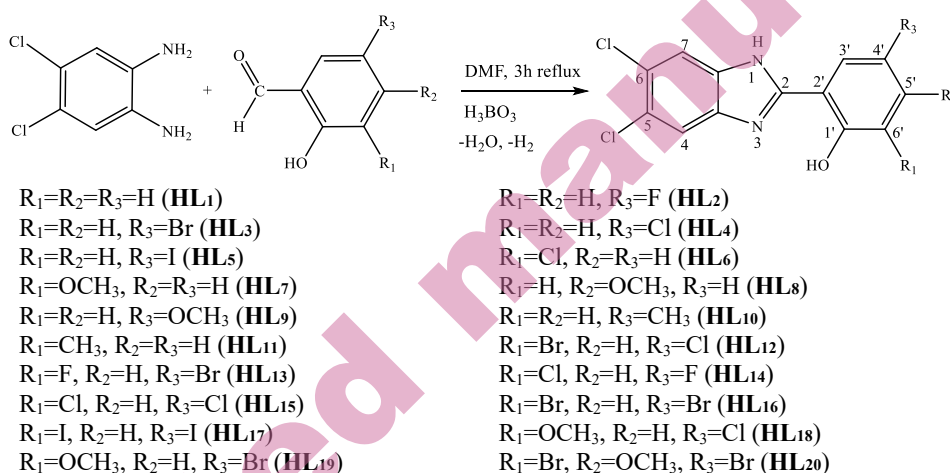
Many researchers in different parts of the world continue their research on benzimidazole derivatives because they have a wide range of biological activities, especially antimicrobial, antiviral, antifungal, anti-inflammatory, proton pump and pancreatic lipase inhibitor, hormone modulator, antihypertensive, antidiabetic, antidepressant, anticoagulant, etc.[10-14] Also, it is known that there is a 5,6-dimethylbenzimidazole moiety that coordinated to a Co(II) ion through the imidazole C=N nitrogen atom in vitamin B12.[15]

Benzimidazole derivatives containing phenol groups, benzimidazolylphenols, are one of the current and widespread research topics, and their results have application potential in many areas. One of the most important features of these compounds is that they form strong chelate complexes with a two-ring structure by coordinating to metals through phenolic OH oxygen and C=N nitrogen atoms. In addition, many studies have been published examining the photophysical properties of these compounds and their complexes with strong fluorescent characteristics.[16,17]

We reported that many benzimidazolyl-phenol derivatives and some of their transition metal complexes exhibited antibacterial and antifungal effect in our previous studies.[18] For example, 2-(5-nitro-1*H*-benzimidazol-2-yl)-bromophenol and its Zn(II), Fe(III) and Cu(II) complexes showed considerable antibacterial activity on *S. aureus* and *S. epidermidis*.[19,20] It is observed that the Cl, Br and NO$_2$ groups in some 5-methoxy-2-(5-substituted-1*H*-benzimidazol-2-yl)-phenols increase the antimicrobial activity toward *S. aureus*, *E. faecalis* and *C. albicans*.[21]

In this study, twenty benzimidazolylphenol derivatives, eighteen of them are new, 5,6-dichloro-1*H*-benzimidazol-2-yl-(4'/5'/6'-substituted)-phenols (**HL₁** – **HL₂₀**, Scheme 1) were synthesized and characterized. The compounds except for **HL₁** and **HL₄** are reported for the first time in this study. The compound 2-(5,6-dichloro-1*H*-benzimidazol-2-yl)phenol (**HL₁**) and its Mn(III), Fe(II), Co(II) and Ni(II) complexes were reported in the literature.[22–24] Additionally, the anticancer effect of a group of compounds, including **HL₁**, was examined, and it was reported

that **HL₁** showed very weak anticancer activity against A549, MDA-MB-231, and PC3 cell lines (IC$_{50}$ value >100 µg mL^{-1} for all three cell types).[25] The anticancer activity of **HL₄** was also investigated, but no significant effect was observed.[26] We also prepared the MCl₂ complexes (M: Co, Ni, Cu, Zn, Pd) of **HL₁** and characterized. In addition, antimicrobial activities of the compounds were tested towards six bacteria and three fungi. The structural characteristics and antimicrobial activity of the compounds were investigated and compared.

R₁=R₂=R₃=H (**HL₁**)   R₁=R₂=H, R₃=F (**HL₂**)
R₁=R₂=H, R₃=Br (**HL₃**)   R₁=R₂=H, R₃=Cl (**HL₄**)
R₁=R₂=H, R₃=I (**HL₅**)   R₁=Cl, R₂=R₃=H (**HL₆**)
R₁=OCH₃, R₂=R₃=H (**HL₇**)   R₁=H, R₂=OCH₃, R₃=H (**HL₈**)
R₁=R₂=H, R₃=OCH₃ (**HL₉**)   R₁=R₂=H, R₃=CH₃ (**HL₁₀**)
R₁=CH₃, R₂=R₃=H (**HL₁₁**)   R₁=Br, R₂=H, R₃=Cl (**HL₁₂**)
R₁=F, R₂=H, R₃=Br (**HL₁₃**)   R₁=Cl, R₂=H, R₃=F (**HL₁₄**)
R₁=Cl, R₂=H, R₃=Cl (**HL₁₅**)   R₁=Br, R₂=H, R₃=Br (**HL₁₆**)
R₁=I, R₂=H, R₃=I (**HL₁₇**)   R₁=OCH₃, R₂=H, R₃=Cl (**HL₁₈**)
R₁=OCH₃, R₂=H, R₃=Br (**HL₁₉**)   R₁=Br, R₂=OCH₃, R₃=Br (**HL₂₀**)

Scheme 1. Synthesis scheme and chemical structures of 5,6-dichloro-1*H*-benzimidazol-2-yl-(4'/5'/6'-substituted)-phenols in the study

EXPERIMENTAL

Chemistry and apparatus

All chemicals and solvents were of reagent grade and they were used without further purification. Information on the chemicals and equipment used is provided as supporting information.

Synthesis of 5,6-dichloro-1H-benzimidazol-2-yl-(4'/5'/6'-substituted)-phenols (HL₁ – HL₂₀)

A modified method developed by us by utilizing two different methods available in the literature was applied in the synthesis of benzimidazolylphenol derivatives.[27,28] An appropriate aldehyde (0.003 mol) and 4,5-dichlorobenzene-1,2-diamine (0.003 mol, 0.531 g) and 0.150 g H₃BO₃ as catalyst were dissolved in 20 mL DMF, and refluxed for 3 h. The reaction mixture was left to cool at room temperature and then poured into 250 mL of water, after which a precipitate formed. It was filtered, dried and crystallized from ethanol after. The compounds were obtained in yields ranging from 65 to 94 %. Physicochemical and spectroscopic data for **HL₁** – **HL₂₀** are given in the supplementary file.

Synthesis of the complex compounds

Appropriate metal salt solutions {0.0075 mol of CoCl₂·6H₂O, NiCl₂·6H₂O, CuCl₂·2H₂O in 10 mL ethanol, K₂PdCl₄ {was obtained by dissolving 1 mmol PdCl₂ (0.177 g) and 2 mmol KCl (0.15 g) in 10 mL MeOH+H₂O mixture (6:4, v/v)}, and ZnCl₂·6H₂O in 10 mL of ethylacetate}

was added to a solution of the **HL₁** (0.210 g, 0.0075 mol) in appropriate solvent (15 mL), and heated to reflux for 3 h. The resulting precipitates were filtered off after cooling the reaction mixture, washed with a very small amount of methanol and water and kept at room temperature to dry.

[Co(**L₁**)₂(H₂O)₂]: Light brown solid. Yield: 71 %; dec. p.: 168 °C; Combustion analysis for $C_{26}H_{18}Cl_4N_4O_4Co$ (FW: 651.19): Calculated. C 47.95, H 2.79, N 8.60; found C 48.42, H 3.04, N 8.48. Magnetic moment, μ_{eff}: 3.47μ_B. Λ_M (DMF, 25 °C, S m² mol⁻¹): 21.3. IR (ATR, cm⁻¹): 3225m,br ν(H₂O+NH), 3107m ν(CH)$_{ar.}$, 1607m ν(C=N), 1599m ν(C=C), 1485m, 1453m, 1372m, 1245m ν(C−O), 1098m, 960m, 864m δ(CH)$_{ar.}$, 813m, 751s ν(C−Cl), 677m, 578m, 545m, 502m ν(Co–O), 462m ν(Co←N), 428m. TGA (t / °C: weight loss, %): 100: 1.1; 150: 5.7; 200: 6.7; 300: 19.4; 400: 53.1; 500: 85.2; 600: 87.5; 700: 89.1; 800: 89.1 (Theoretical value of CoO: 11.5 %). Fluorescence spectra (EtOH, c = 1×10⁻⁴ mol L⁻¹, λ_{max}/ nm): 469m.

[Ni(**L₁**)₂]·2H₂O: Light brown solid. Yield: 73 %; dec. p.: 165 °C; Combustion analysis for $C_{26}H_{18}Cl_4N_4O_4Ni$ (FW: 650.95): Calculated. C 47.97, H 2.79, N 8.61; found C 48.33, H 2.96, N 8.44. Magnetic moment, μ_{eff}: 2.05 μ_B. Λ_M (DMF, 25 °C, S m² mol⁻¹): 31.5. IR (ATR, cm⁻¹): 3356m ν(OH), 3269m ν(NH), 3068m ν(CH)$_{ar.}$, 1609m ν(C=N), 1595m ν(C=C), 1503m, 1456m, 1387m, 1246m ν(C−O), 1103m, 1039m, 854m δ(CH)$_{ar.}$, 815m, 754s ν(C−Cl), 680m, 616m, 537m, 504m ν(Ni–O), 449m ν(Ni←N), 416m. TGA (t / °C: weight loss, %): 100: 5.8; 150: 6.0; 200: 6.5; 300: 18.2; 400: 51.6; 500: 86.5; 600: 88.2; 700: 88.8; 800: 88.8 (Theoretical value of NiO: 11.5 %). Fluorescence spectra (EtOH, c = 1×10⁻⁴ mol L⁻¹, λ_{max}/ nm): 417sh, 462m.

[Cu(**L₁**)₂]·H₂O: Brown solid. Yield: 80 %; dec. p.: 332 °C; Combustion analysis for $C_{26}H_{16}Cl_4N_4O_3Cu$ (FW: 637.80): Calculated. C 48.96, H 2.53, N 8.78; found C 48.60, H 2.54, N 8.41. Magnetic moment, μ_{eff}: 1.62 μ_B. Λ_M (DMF, 25 °C, S m² mol⁻¹): 7.1. IR (ATR, cm⁻¹): 3357m,br ν(H₂O+NH), 3130m,br, 3054w ν(CH)$_{ar.}$, 1617m ν(C=N), 1588m ν(C=C), 1556m, 1451m, 1355m, 1244sν(C–O), 1197m, 1100m, 975m, 868m δ(CH)$_{ar.}$, 759m, 742m ν(C−Cl), 691m, 573m, 546m, 503m ν(Cu–O), 443m ν(Cu←N), 420m. TGA (t / °C: weight loss, %): 100: 2.7; 150: 3.3; 200: 6.3; 300: 18.0; 400: 49.5; 500: 85.5; 600: 87.3; 700: 87.5; 800: 87.7 (Theoretical value of CuO: 12.5 %). Fluorescence spectra (EtOH, c = 1×10⁻⁴ mol L⁻¹, λ_{max}/ nm): 469w,br.

[Zn(**L₁**)Cl(H₂O)]·2H₂O: Dirty white solid. Yield: 71 %; dec.p.: 270 °C; Combustion analysis for $C_{13}H_{13}Cl_3N_2O_4Zn$ (FW: 433.02): Calculated. C 36.06, H 3.03, N 6.47; found C 35.84, H 2.88, N 6.32. Λ_M (DMF, 25 °C, S m² mol⁻¹): 45.8. IR (ATR, cm⁻¹): 3365m,br ν(OH), 3203m,br ν(NH), 3042w ν(CH)$_{ar.}$, 1620m ν(C=N), 1609m ν(C=C), 1558m, 1483m, 1456m, 1321m, 1233s ν(C–O), 1147m, 969m, 856m δ(CH)$_{ar.}$, 740s ν(C−Cl), 692m, 577m, 541s, 505m ν(Zn–O), 443m ν(Zn←N), 421m. ¹H-NMR (500 MHz, DMSO-d₆, δ): 12.81 (*brs*, 1H, NH), 7.89 (*brs*, 2H, H4+H7), 7.84 (*dd*, 1H, J₁ = 7.9, J₂ = 1.6, H3'), 7.15 (*dt*, 1H, J₁ = 8.3, J₂ = 1.4, H4'), 6.71 (*dd*, 1H, J₁ = 7.7, J₂ = 3.7, H6'), 6.52 (*td*, 1H, J₁ = 7.2, J₂ = 7.1, J₃ = 1.2, H5'). TGA (t / °C: weight loss, %): 100: 8.6; 150: 11.7; 200: 16.4; 300: 25.1; 400: 53.5; 500: 79.4; 600: 82.2; 700: 82.4; 800: 82.5 (Theoretical value of ZnO: 18.8 %). Fluorescence spectra (EtOH, c = 1×10⁻⁴ mol L⁻¹, λ_{max}/ nm): 425sh, 450m,br.

[Pd(**L₁**)₂]·2H₂O: Soil colored solid. Yield: 66 %; dec. p. >350 °C; Combustion analysis for $C_{26}H_{18}Cl_4N_4O_4Pd$ (FW: 698.70): Calculated. C 44.41, H 3.01, N 7.21; found C 44.70, H 2.60, N 8.02. Λ_M (DMF, 25 °C, S m² mol⁻¹): 14.3. IR (ATR, cm⁻¹): 3269m,br ν(NH+OH₂), 3117w ν(CH)$_{ar.}$, 1602m ν(C=C), 1588m ν(C=N), 1531m, 1476m, 1310m, 1239s ν(C–O), 1144m, 1034m, 969m, 870m δ(CH)$_{ar.}$, 753s ν(C−Cl), 702m, 672m, 568m, 503m ν(Pd–O), 443m ν(Pd←N). ¹H-NMR (500 MHz, DMSO-d₆, δ): 13.43 (*s*, 1H, NH), 7.94 (*brs*, 1H, H7), 7.87 (*s*, 1H, H4), 7.68 (*dt*, 1H, J₁ = 8.0, J₂ = 1.7, H5'), 7.45 (*dt*, 1H, J₁ = 7.8, J₂ = 7.1, J₃ = 1.0, H4'), 7.22

(*d*, 1H, J = 7.6, H6'), 7.05 (*dt*, 1H, J$_1$ = 8.0, J$_2$ = 1.0, H3'). TGA (t / °C: weight loss, %): 100: 5.4; 150: 5.7; 200: 6.1; 300: 19.9; 400: 49.7; 500: 74.6; 600: 77.3; 700: 81.1; 800: 81.2 (Theoretical value of PdO: 17.5 %). Fluorescence spectra (EtOH, *c* = 1×10^{-4} mol L^{-1}, λ_{max}/ nm): 415sh, 459m.

Determination of antimicrobial activity

Antibacterial activity of samples was studied *in vitro* with microbroth dilution technique against *Staphylococcus aureus* ATCC 29213 (meticillin susceptible *Staphylococcus aureus*, MSSA)*, Enterococcus facealis* ATCC 29212, *Escherichia coli* ATCC 25922, *Klebsiella pneumonia* ATCC 4352, *Pseudomonas aeruginosa* ATCC 27853, *Staphylococcus epidermidis* ATCC 12228. Antifungal activity was assayed *in vitro* against *Candida albicans* ATCC 10231, *Candida parapsilosis* ATCC 22019 and *Candida tropicalis* ATCC 750. The evaluation of antibacterial and antifungal activity was done using micro broth dilution technique according to the Clinical Laboratory Standards Institute (CLSI) guidance[29,30] as detailed in previous studies.[21]

The samples were evaluated for their antibacterial and antifungal potency against members of Gram-negative bacteria, Gram-positive bacteria, and Candida spp. As reference compounds, Ciprofloxacin for antibacterial assays, and Amphotericin B for antifungal assays were preferred.

X-Ray diffraction analysis

Suitable crystals of **HL₁₈** were selected for data collection which was performed on a D8-QUEST diffractometer equipped with a graphite-monochromatic Mo-K$_\alpha$ radiation at 296 K. The structure was solved by direct methods using SHELXS-2013[31] and refined by full-matrix least-squares methods on F^2 using SHELXL-2013.[32] All non-hydrogen atoms were refined with anisotropic parameters. The following procedures were implemented in our analysis: data collection: Bruker APEX2;[33] program used for molecular graphics were as follow: MERCURY programs;[34] software used to prepare material for publication: WinGX.[35]

RESULTS AND DISCUSSION

Crystal structure of **HL₁₈**

Crystal data and structure refinement parameters related **HL₁₈** are given in Table I. Some important data on bond distances and bond angles are shown in Table SI, and hydrogen bond parameters are shown in Table II. Molecular structure of **HL₁₈** is shown in Fig. 1, and the molecular planes and intermolecular hydrogen bonds in Figure S-1.

HL₁₈ crystallized in the monoclinic system. The C−O bond length of 1.353 Å, indicate that the bond has a typical phenolic C−O length. It is clearly seen that there is an intramolecular hydrogen bond with N2···H1A distance 1.86 Å. There is also intermolecular hydrogen bond in the molecule. There appear to be four different intermolecular hydrogen bonds in **HL₁₈**: C14−H14A···O1 (2.36 Å), N2−H2A···Cl3 (2.21 Å), O1−H1···Cl3 (2.24 Å) and O2−H2B···Cl3 (2.23 Å). These hydrogen bonds affect the solubility and stability of the molecule.
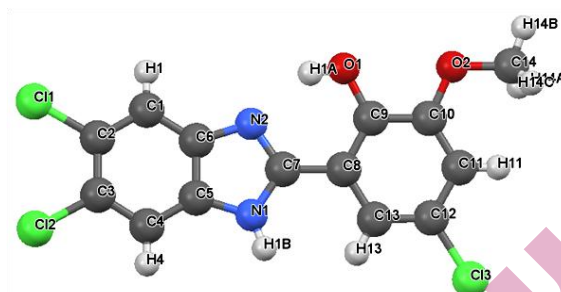
Fig. 1. Molecular structure of **HL₁₈** showing the atom numbering scheme.

TABLE I. Crystal data and structure refinement parameters.

Empirical formula	$C_{14}H_9Cl_3N_2O_2$
Formula weight	343.58
Crystal system	Monoclinic
Space group	*C2/c*
a (Å)	27.298 (4)
b (Å)	7.3699 (9)
c (Å)	14.1238 (18)
β (º)	100.596 (4)
V (Å³)	2793.1 (6)
Z	8
D_c (g cm⁻³)	1.634
μ (mm⁻¹)	0.66
θ range (º)	2.9-26.5
Measured refls.	28774
Independent refls.	3224
R_{int}	0.058
S	1.05
R1/wR2	0.049/0.107
$\Delta\rho_{max}/\Delta\rho_{min}$ (eÅ⁻³)	0.26/-0.25
CCDC	2194768

TABLE II. Hydrogen-bond parameters (Å, º)

D−H···A	D−H	H···A	D···A	D−H···A
O1—H1A···N2	0.82	1.86	2.594	148
C14—H14A···O1	0.97	2.36	3.108 (4)	134
N2—H2A···Cl3ⁱ	0.86	2.21	3.063 (3)	176
O1—H1···Cl3	0.82	2.24	3.047 (3)	166
O2—H2B···Cl3ⁱⁱ	0.82	2.23	3.045 (3)	173

Symmetry codes: (i) −x, y+1/2, −z+1/2; (ii) −x+1, y+1/2, −z+1/2

General properties

In this study, twenty 5,6-dichlorobenzimidazolyl-phenol derivatives were obtained, eighteen of which are reported here for the first time. In addition, five

related transition metal complexes were obtained by allowing **HL₁** to react with Co(II), Ni(II), Cu(II), Zn(II) and Pd(II) ions at a molar ratio of 1:2 metal:ligand. This ratio is 1:1 in the Zn(II) complex obtained and 1:2 in the others. Despite many attempts, no single crystal sample suitable for X-ray study could be obtained from the complexes.

The molar conductivity values of all complexes in DMF are below 50 S m^2 mol^{-1}, and these values indicate non-ionic structures according to Geary.[36]

The magnetic moment value of the Ni(II) complex was found to be 2.05 μ_B, which is lower than the 2.83 μ_B expected for octahedral or tetrahedral geometries, which are paramagnetic structures that the d^8 ion with two unpaired electrons may have. Such low values are generally thought to be due to the distorted geometry between the tetrahedral and square planar systems, called quasi-tetrahedral.[37] The magnetic moment value found as 3.47 μ_B for the Co(II) complex can be considered as evidence that the five-coordinated d^7 complex is in a high-spin structure (three unpaired electrons). The geometry of the central ion may be octahedral. The magnetic moment value of the Cu(II) complex at room temperature was found to be 1.62 μ_B, indicating the formation of a monomeric complex. Although this value is lower than the theoretical value of 1.71 μ_B for the Cu(II) ion with d^9 electronic configuration, it remains within acceptable limits due to the influence of various factors.

FT-IR spectra

FT-IR spectral data are given at experimental section (for the complexes) and supplementary information (for **HL₁** – **HL₂₀**). In the IR spectra of most of the benzimidazolyphenol derivatives, strong or medium bands are seen in the range of 3243 – 3420 cm^{-1}. These bands are related to the combination of ν(O–H) and ν(N–H) frequencies and arises from the formation of intramolecular hydrogen bonding between C=N nitrogen and OH hydrogen atoms.[38,39] This band observed at 3333 cm^{-1} in **HL₁** disappeared as a result of the coordination of phenolic oxygen atom with the formation of the complexes.[40]

The stretching and out-of-plane bending modes [ν(C–H) and δ(C–H)] of the aromatic rings are detected at the 3117 – 3042 cm^{-1} and 870 – 800 cm^{-1} wavenumber regions, respectively, for all the compounds. The stretching frequencies of the aromatic C=C and the imidazole C=N groups are identified at the ranges of 1577 – 1609 cm^{-1} and 1614 – 1657 cm^{-1}, respectively, as expected. In the spectra of **HL₁**, the medium band at 1256 cm^{-1} can be assigned to ν(C–O) of the phenolic group and it shifted to the range of 1233 – 1246 cm^{-1} in the complexes as a result of the phenolic oxygen atom coordination. The bands of ν(C–O) were determined in the range of 1182 – 1273 cm^{-1} in the spectra of other benzimidazolylphenol derivatives (**HL₂** – **HL₂₀**).

The C–Cl stretching vibrations are seen at the range of 710 – 796 cm^{-1} as medium bands in all of the compounds.[41] In the iodine-containing compounds,

HL5 and **HL17**, the C–I vibrations bond can be detected around 550 cm^{-1}; in the bromine-containing compounds, **HL3**, **HL13**, **HL16**, **HL19** and **HL20**, the medium bands between 550 and 600 cm^{-1} can be attributed to ν(C–Br). The ν(C–F) is expected to give a band above 1000 cm^{-1} in derivatives containing fluorine atom (**HL2**, **HL13** and **HL14**); however it is difficult to detect the band of this bond due to interference with the vibrations of other bonds.[42]

The emergence of new bands of medium intensity around 503 cm^{-1} can be assigned to the ν(M–OC) vibration frequencies resulting due to phenolic oxygen atom coordination.[43] It was evaluated that the new bands appearing in the complexes between 443 – 462 cm^{-1} belong to the stretching vibration mode of the M←N bond formed as a result of the coordination of the C=N nitrogen atom.[44] The coordination of the C=N nitrogen atom can also be associated with the shift of the 1639 cm^{-1} band of the ligand to the lower wavenumbers in the IR spectra of the complexes to 1602 – 1620 cm^{-1} range. The broad bands with medium characteristics between 3365 and 3225 cm^{-1} in the complexes mightily support the presence of the H$_2$O molecules.

It is known that the keto-enol structure is found in benzimidazolylphenol type compounds.[16] According to the IR spectral data, **HL3**, **HL4**, **HL12** – **HL15**, **HL17** and **HL20** compounds also have keto form in the solid state (Fig. 2). In other words, there is a keto-enol mixture in these compounds. The weak or medium bands at 1662 – 1723 cm^{-1} range are considered to arise from the C=O bond in the keto form of the compounds in the solid state.
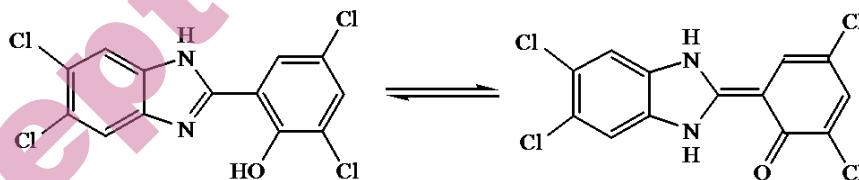

Fig. 2. Keto-enol tautomer structures of **HL15**

NMR spectra

^{1}H-NMR spectral data of **HL1** – **HL20** are given in the supplementary information, and those of diamagnetic complexes are given in the experimental section. In the ^{1}H-NMR spectra of the compounds, signals of the NH and OH protons were detected at the 13.88 – 11.64 ppm range, and aromatic ring protons appeared in the range of 7.0 to 8.5 ppm. In ^{1}H-NMR spectra, whether salicylic OH protons are removed or not can be evaluated in relation to whether complexation occurs via the oxygen atom. Indeed, the absence of OH proton in both Zn(II) and Pd(II) complexes of **HL1** shows that phenolic proton is removed and the oxygen atom is coordinated. While the chemical shift values of the ligand protons in Pd(II) complex were detected at significantly higher ppm values (downfield shift), the

shifts in Zn(II) complex were observed to be weaker compared to the Pd(II) complex, albeit in the same direction.

Although the keto form of some benzimidazolylphenols is dominant in the solid state according to IR data, the detection of OH protons shows that the enol structure is dominant in DMSO (or organic solvents) in the NMR spectra of all benzimidazolylphenol derivatives.

Thermogravimetric analysis

Thermal analysis data of the complexes are outlined in Experimental. The samples were heated from room temperature up to 800 °C in air atmosphere. Thermogravimetric analysis values provide important clues, especially explaining the status of H_2O molecules. It is known that lattice H_2O molecules removed up to 100 °C and coordinated H_2O molecules up to 200 °C. The 5.7 % mass loss seen in thermal analysis of the Co(II) complex around 150 °C can be considered as an indication of presence of two moles of coordinated H_2O considering the fact that two moles of H_2O in the complex corresponds to a theoretical mass of 5.5 %. The mass losses of 5.8 and 5.4 % in Ni(II) and Pd(II) complexes up to 100 °C, respectively, can be explained by the presence of two moles of lattice H_2O in both complexes (theoretical values are 5.5 and 5.15 % for Ni(II) and Pd(II) complexes, respectively). In addition, the absence of significant mass loss in these complexes between 100 and 200 °C (0.2 and 0.3 %, respectively for Ni(II) and Pd(II) complexes) can be attributed to the absence of coordinated H_2O molecules. In the Zn(II) complex, the mass losses of 8.6 % up to 100 °C and 4.3 % between 100 and 200 °C are evaluated to be related to two moles lattice and one mole coordinated H_2O molecules, respectively.

According to TGA data, the Zn(II) complex begins to decompose above 200 °C and the others above 300 °C. The different thermal behavior of the Zn(II) complex may be related to its different M:L ratio from the others with a ratio of 1:1. The fact that a greater mass loss occurs in the Zn(II) complex above 200 °C, unlike the others, can be interpreted that the chlorine atom starts leaving as HCl the complex around this temperature and completely remove up to 300 °C (totally 25.1 % mass loss).

It is possible to suggest that above 500 °C all complexes are completely decomposed and metal oxide forms begin to form. The mass ratios remaining from the complexes after complete dissociation are consistent with the theoretical mass ratios calculated for metal oxides.

Fluorescence spectra

The emission maximum data of the compounds are given in the experimental section (for the complexes) and supplementary information (for **HL₁** – **HL₂₀**). It was observed that **HL₁** emits strong fluorescence at 466 nm. Among the compounds, the highest emission spectrum wavelength belongs to **HL₉** (4-

methoxy derivative), which has dual fluorescence characteristic, with a value of 508 nm. **HL₉** also emits strongly at 389 nm. The lowest emission spectrum wavelength belongs to **HL₈** (5-methoxy derivative) with a value of 452 nm (Fig. 3). **HL₆**, which has a chlorine substitution at 2-position on the phenol ring, is another compound that exhibits a lower emission wavelength (blueshift) according to **HL₁**, with a value of 463 nm. A redshift effect is observed in all compounds except **HL₆** and **HL₈**. Based on these observations, it can be concluded that substitutions generally cause redshift.
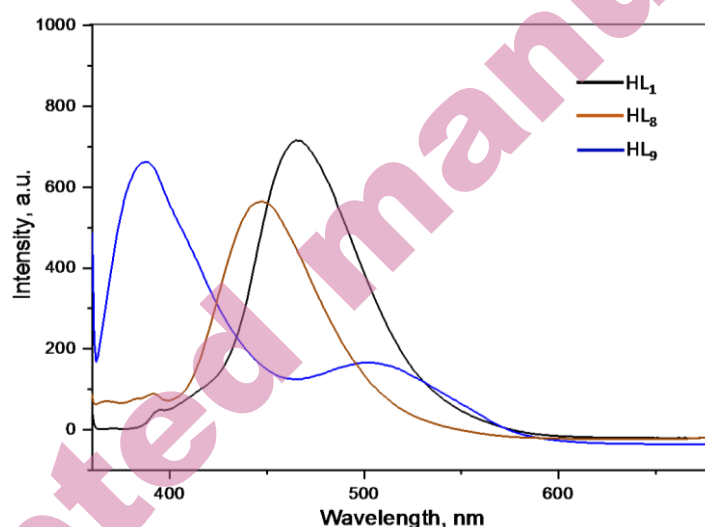

Fig. 3. Comparative fluorescence spectra of **HL₁** and its derivatives with the lowest and highest emission wavelength values

While there is no significant shift in the complexes relative to the ligand, there is a significant decrease (or quenching effect) in the fluorescence intensity. The Zn(II) complex, which emits light at 450 nm, differs from the others by showing a red shift. It is also worth noting that the decrease in fluorescence intensity in the Cu(II) complex is greater than the others (Fig. 4).
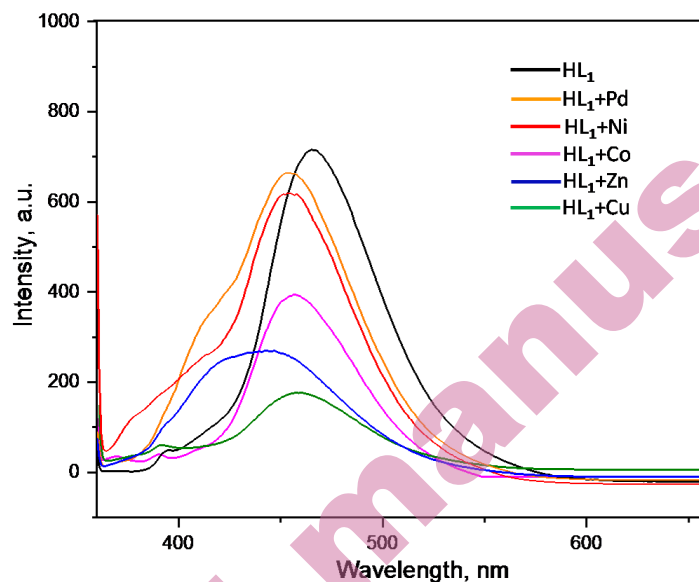
Fig. 4. The comparative fluorescence spectra of **HL₁** and its complexes

Considering all the analytical, physicochemical and spectroscopic data described above, the proposed structures in Fig. 5 can be suggested for the complexes.
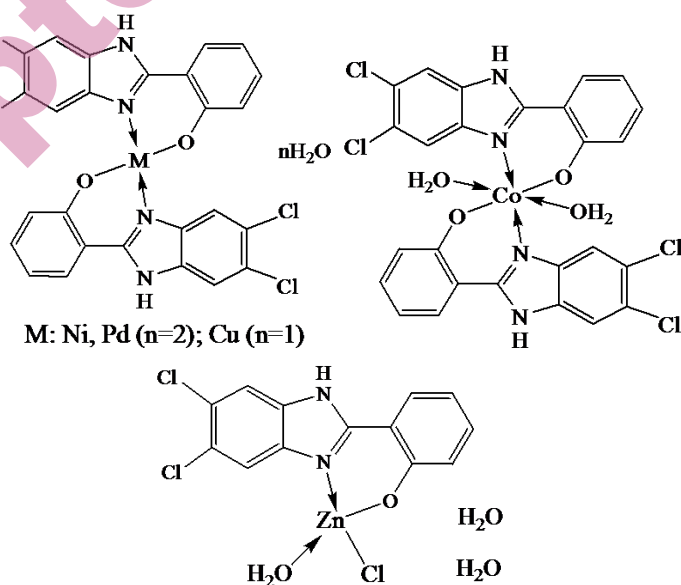

Fig. 5. Suggested coordinations for the complexes in the study

Antimicrobial activity

The results of the in vitro antibacterial and antifungal activities of the compounds and the values of the antibiotic and antifungal drugs given for comparison are presented in Table III as MIC (minimum inhibitory concentration).

TABLE III. *In vitro* antimicrobial activity of the compounds (MIC, $\mu g\ mL^{-1}$)

Compound	Microorganisms								
	$Sa^{*,a}$	Se^a	Ec^b	Kp^b	Pa^b	Pm^b	Ca	Cp	Ct
HL₁	**19.5**	**39**	78	625	$-^c$	312	-	625	625
HL₂	**19.5**	156	312	156	-	312	-	**39**	625
HL₃	**19.5**	156	312	625	-	312	-	156	625
HL₄	**39**	**39**	625	156	-	625	-	312	312
HL₅	156	312	625	625	625	312	625	1250	1250
HL₆	78	156	156	156	-	156	39	156	312
HL₇	156	**9.75**	312	625	-	312	-	312	312
HL₈	156	156	312	312	-	625	-	312	625
HL₉	156	78	156	625	-	312	-	625	625
HL₁₀	**19.5**	78	312	156	-	625	-	312	625
HL₁₁	**39**	**19.5**	156	312	-	312	-	156	625
HL₁₂	156	312	625	625	1250	625	1250	1250	1250
HL₁₃	312	156	625	625	625	625	1250	1250	625
HL₁₄	312	156	1250	625	1250	625	1250	625	625
HL₁₆	156	312	1250	625	1250	312	1250	625	625
HL₁₆	312	156	1250	1250	1250	312	1250	1250	625
HL₁₇	156	156	625	625	1250	312	625	625	1250
HL₁₈	312	312	625	625	1250	625	1250	1250	1250
HL₁₉	156	156	625	625	1250	625	625	625	1250
HL₂₀	312	156	625	1250	1250	625	625	1250	1250
HL₁+Co(II)	625	312	1250	625	625	625	625	625	1250
HL₁+Ni(II)	312	312	1250	1250	1250	312	1250	1250	1250
HL₁+Cu(II)	312	312	1250	625	1250	312	625	1250	625
HL₁+Zn(II)	156	156	2500	1250	1250	312	1250	625	1250
HL₁+Pd(II)	625	156	625	1250	625	312	1250	625	1250
References**	0.25	0.0625	0.0156	0.0078	1.0	0.0156	0.5	1.0	1.0

* Sa - Staphylococcus aureus ATCC 29213; Se- Staphylococcus epidermidis ATCC 12228; Ec - Escherichia coli ATCC 25922; Kp - Klebsiella pneumoniae ATCC 4352; Pa - Pseudomonas aeruginosa ATCC 27853; Pm - Proteus mirabilis ATCC 14153; Ca - Candida albicans ATCC 10231; Cp - Candida parapsilosis ATCC 22019; Ct - Candida tropicalis ATCC 750; [a] - Gram positive; [b] - Gram negative; [c] - : No antimicrobial effect at 5000 $\mu g\ mL^{-1}$ and lower dilutions; ** - Ciprofloxacin and Amphotericin B were used for bacteria and fungi, respectively.

When the table is examined, it is noted that the first eleven compounds (**HL₁** to **HL₁₁**) show better compared to the other compounds and selective activity against some microorganisms. The common feature of these compounds is that they are all mono substituted derivatives of **HL₁**. It can be said that all mono

substituted derivatives show selective activity especially against Gram positive bacteria, *S. aureus* and *S. epidermidis*. The activity of **HL7** (6´-methoxy derivative) against *S. epidermidis* is remarkable with 9.75 µg mL^{-1}. However, another noteworthy finding is that disubstituted derivatives of **HL1** (**HL12** to **HL20**) are also moderately or weakly effective against all microorganisms (non-selective general activity).

In our previous studies, it was determined that various benzimidazole derivatives exhibited selective activity, particularly against Gram-positive bacteria and some fungal species.[18,45] It was observed that benzimidazolyphenol derivatives containing methoxy and nitro/bromine/chlorine groups were distinguished from others by their activity against Gram-positive bacteria such as *S. aureus* and also *C. albicans*.[41]

No significant antimicrobial activity was detected in the complexes according to the ligand. The only striking feature is that the complexes showed slightly higher antifungal activity against *C. albicans*, where the ligand showed no activity. It can be assumed that the complexes form stable chelates with the ligands at a 1:2 M:L ratio, thus limiting the activity of the ligands and therefore lowering the activity compared to the ligand. The relatively high activity of the Zn(II) complex, with a 1:1 M:L ratio, against Gram-positive bacteria may be attributable to its structural feature. A possible mechanism is that the Zn(II) complex, thought to bind one mole of water, releases water upon contact with bacteria and binds to their proteins.

CONCLUSION

In this study, 2-(5,6-dichloro-1*H*-benzimidazol-2-yl)phenol (**HL1**) and its nineteen derivatives with different substituents on the phenol ring were obtained and their structural properties were investigated. Structure of **HL18** was investigated by X-ray single crystal spectroscopy, also. Additionally, M(II) complexes (M: Co, Ni, Cu, Zn and Pd) of **HL1** were obtained and various physicochemical and spectroscopic properties were investigated. It was found that all complexes have non-electrolytic properties and the M:L ratios are 1:1 in the Zn(II) complex and 1:2 in the other complexes. Fluorescence spectral studies show that in all compounds except HL6 and HL8, the substitution results in a shift of the fluorescence emission to lower wavelengths (redshift) compared to **HL1**. The zinc(II) complex showed a greater redshift effect compared to the other complexes. After characterization, antibacterial and antifungal activity of all the compounds was evaluated against six bacteria and three fungi. Compounds **HL1** to **HL11** (**HL1** and its monosubstituted derivatives) show better compared to the other compounds and selective activity against some microorganisms. Another noteworthy result is that the complexes of **HL1** show weak activity against *C. albicans*, against which **HL1** itself is inactive. It was observed that the Zn(II) complex showed relatively

higher activity against *S. aureus* and *S. epidermidis* (Gram positive bacteria) compared to the other complexes.

SUPPLEMENTARY MATERIAL

И З В О Д

СПЕКТРАЛНА КАРАКТЕРИЗАЦИЈА И ИСПИТИВАЊЕ АНТИМИКРОБНЕ АКТИВНОСТИ 5,6-ДИХЛОРО-1*H*-БЕНЗИМИДАЗОЛ-2-ИЛ-(4'/5'/6'-СУПСТИТУИСАНИХ)ФЕНОЛА (HL₁ – HL₂₀) И Co(II), Ni(II), Cu(II), Zn(II) И Pd(II) КОМПЛЕКСА СА HL₁

AYDIN TAVMAN[1], DEMET GURBUZ[2], MAYRAM HACIOGLU[3], ADEM CINARLI[2], ONUR SAHIN[4] и A. SEHER BIRTEKSOZ TAN[3]

[1]Istanbul University-Cerrahpaşa, Faculty of Engineering, Department of Chemistry, Inorganic Chemistry Division, 34320 Avcilar, Istanbul, Türkiye, [2]Istanbul University-Cerrahpaşa, Faculty of Engineering, Department of Chemistry, Organic Chemistry Division, 34320 Avcilar, Istanbul, Türkiye, [3]Istanbul University, Faculty of Pharmacy, Department of Pharmaceutical Microbiology, 34452 Beyazit, Istanbul, Türkiye, [4]Sinop University, Faculty of Health Sciences, Department of Occupational Health and Safety, 57000 Sinop, Türkiye.

5,6-Дихлоро-1*H*-бензимидазол-2-ил-(4'/5'/6'-супституисани)феноли (HL₁–HL₂₀) и MCl₂ комплекси (M: Co, Ni, Cu, Zn, Pd) са HL1 синтетисани су и окарактерисани различитим физичко-хемијским и спектроскопским методама, као што су елементална анализа, термогравиметријска анализа, FTIR, NMR и флуоресцентна спектроскопија. Структуре комплекса потврђене су и мерењем моларне проводљивости и магнетног момента. HL₁ једињење се координовало као бидентатни, монобазни хелатни лиганд са NO донорским атомима у свим комплексима. Утврђено је да су сви комплекси неелектролити, при чему је однос метала и лиганда (M:L) 1:1 у Zn(II) комплексу и 1:2 у осталим комплексима. Кристална структура HL₁₈ је, такође, испитивана, при чему је у оба молекула уочено присуство интра- и интермолекулских водоничних веза. На основу података добијених флуоресцентном спектроскопијом, супституенти у положају 4 изазвали су померање максимума емисије ка нижим таласним дужинама (црвено померање) у поређењу са HL₁, док су супституенти у положају 3 и 5 узроковали плаво померање. Zn(II) комплекс је показао израженије црвено померање у односу на друге комплексе. Поред тога, антимикробна активност једињења је испитивана према шест бактеријских и три гљивичне врсте. Примећено је да HL₁ и његови моносупституисани деривати (HL₁–HL₁₁) показују селективну активност, посебно према Грам-позитивним бактеријама *S. aureus* и *S. epidermidis*. Zn(II) комплекс је показао релативно већу активност према Грам-позитивним бактеријама у поређењу са осталим комплексима.

REFERENCES

1. M. Rasschaert, D. Schrijvers, J. van den Brande, J. Dyck, J. Bosmans, K. Merkle, J. B. Vermorken, *Br. J. Cancer* **96** (2007) 1692 (https://doi.org/10.1038/sj.bjc.6603776)
2. M. Montillo, F. Ricci, A. Tedeschi, E. Vismara, E. Morra, *Expert Rev. Hematol.* **3** (2010) 131 (https://doi.org/10.1586/ehm.10.7)
3. C. S. P. Sastry, P. Y. Naidu, S. S. N. Murty, *Talanta* **44** (1997) 1211 (https://doi.org/10.1016/S0039-9140(97)83117-7)
4. C. Delescluse, M. P. Piechock, N. Ledirac, R. H. Hines, R. Li, X. Gidrol, R. Rahmani, *Biochem. Pharmacol.* **61** (2001) 399 (https://doi.org/10.1016/S0006-2952(00)00562-1)
5. K. K. Mothilal, C. Karunakaran, A. Rajendran, R. Murugesan, *J. Inorg. Biochem.* **98** (2004) 322 (https://doi.org/10.1016/j.jinorgbio.2003.10.017)
6. E. J. Cardoso, A. F. Luna, J. P. Urizar, *Acta Tropica* **92** (2004) 237 (https://doi.org/10.1016/j.actatropica.2004.08.003)
7. M. Savlik, P. Polaskova, B. Szotakova, J. Lamka, L. Skalova, *Res. Vet. Sci.* **79** (2005) 139 (https://doi.org/10.1016/j.rvsc.2004.10.007)
8. R. G. Almeida, J. C. Florio, H. S. Spinosa, M. M. Bernardi, *Neurotoxicol. Teratol.* **24** (2002) 255 (https://doi.org/10.1016/S0892-0362(02)00203-9)
9. J. Gronvold, T. S. Svendsen, H. O. Kraglund, J. Bresciani, J. Monrad, *Vet. Parasitol.* **124** (2004) 91 (https://doi.org/10.1016/j.vetpar.2004.06.003)
10. B. Pathare, T. Bansode, *Results Chem.* **3** (2021) 100200 (https://doi.org/10.1016/j.rechem.2021.100200)
11. S. R. Brishty, M. J. Hossain, M. U. Khandaker, M. R. I. Faruque, H. Osman, S. M. A. Rahman, *Front. Pharmacol.* **12** (2021) 762807 (https://doi.org/10.3389/fphar.2021.762807)
12. G. R. Morais, E. Palma, F. Marques, L. Gano, M. C. Oliveira, A. Abrunhosa, H. V. Miranda, A. Paulo, T. F. Outeiro, I. Santos, *J. Heterocycl. Chem.* **54** (2015) 255 (https://doi.org/10.1002/jhet.2575)
13. R. Sharma, A. Bali, B. Chandhari, *Bioorg. Med. Chem. Lett.* **27** (2017) 3007 (https://doi.org/10.1016/j.bmcl.2017.05.017)
14. A. S. Alpan, S. Parlar, L. Carlino, A. H. Tarikogullari, V. Alptüzün, H. S. Güneş, *Bioorg. Med. Chem.* **21** (2013) 4928 (https://doi.org/10.1016/j.bmc.2013.06.065)
15. R. Bonnett, *Chem. Rev.* **63** (1963) 573 (https://doi.org/10.1021/cr60226a002)
16. W. Y. Zhu, K. Liu, X. Zhang, *Sens. Diagn.* **2** (2023) 665 (https://doi.org/10.1039/D3SD00020F)
17. R. Sathyanarayana, V. Kumar, G. H. Pujar, B. Poojary, M. K. Shankar, S. Yallappa, *J. Photochem. Photobiol. A: Chem.* **402** (2020) 112751 (https://doi.org/10.1016/j.jphotochem.2020.112751)
18. A. Tavman, D. Gürbüz, A. A. Karaçelik, D. N. Çolak, D. Efe, A. Cinarli, *Rev. Roum. Chim.* **69** (2024) 201 (https://doi.org/10.33224/rrch.2024.69.3-4.10)
19. A. Tavman, I. Boz, A. S. Birteksöz, *Spectrochim. Acta* **A77** (2010) 199 (https://doi.org/10.1016/j.saa.2010.05.008)
20. A. Tavman, I. Boz, A. S. Birteksöz, A. Cinarli, *J. Coord. Chem.* **63** (2010) 1398 (https://doi.org/10.1080/00958971003789835)
21. A. Tavman, D. Gürbüz, S. Oksüz, A. Cinarli, *Mor. J. Chem.* **6** (2018) 328 (https://doi.org/10.48317/IMIST.PRSM/morjchem-v6i2.7909)

22. L. Wang, C. X. Zhang, J. Q. Zhao, *Chinese J. Struct. Chem.* **33** (2014) 1479 (https://caod.oriprobe.com/articles/43884889/Synthesis__Structure_and_Catalytic_A ctivity_of_a_M.htm)

23. M. Haghverdi, A. Tadjarodi, N. Bahri-Laleh, M. N. Haghighi, *J. Coord. Chem.* **71** (2018)1180 (https://doi.org/10.1080/00958972.2018.1446527)

24. M. Haghverdi, A. Tadjarodi, N. Bahri-Laleh, M. N. Haghighi, *Appl. Organomet. Chem.* **32** (2018) e4015 (https://doi.org/10.1002/aoc.4015)

25. T. K. C. Huynh, T. H. A. Nguyen, T. C. T. Nguyen, T. K. D. Hoang, *RSC Adv.* **10** (2020) 20543 (https://doi.org/10.1039/D0RA02282A)

26. M. M. Karpinska, J. Matysiak, A. Niewiadomy, *Arch. Pharm. Res.* **34** (2011) 1639 (https://doi.org/10.1007/s12272-011-1008-0)

27. H. F. Ridley, G. W. Spickett, G. M. Timmis, *J. Het. Chem.* **2** (1965) 453 (https://doi.org/10.1002/jhet.5570020424)

28. Z. Karimi-Jaberi, M. Amir, *J. Chem.* **9** (2012) 167 (https://doi.org/10.1155/2012/793978)

29. M27-A3: *Clinical and Laboratory Standards Institute (CLSI)*, *Reference Method for Broth Dilution Antifungal Susceptibility Testing of Yeasts*; Approved Standard-Third Edition. (2012)

30. M100-Ed.31: *Clinical and Laboratory Standards Institute (CLSI), Performance Standards for Antimicrobial* (2021)

31. G. M. Sheldrick, *Acta Cryst.* **A64** (2008) 112 (https://doi.org/10.1107/S0108767307043930)

32. G. M. Sheldrick, *Acta Cryst.* **C71** (2015) 3 (https://doi.org/10.1107/S2053229614024218)

33. APEX2: Bruker AXS Inc. Madison Wisconsin USA (2013)

34. C. F. Macrae, I. J. Bruno, J. A. Chisholm, P. R. Edgington, P. McCabe, E. Pidcock, L. Rodriguez-Monge, R. Taylor, J. van de Streek, P. A. Wood, *J. Appl. Cryst.* **41** (2008) 466 (https://doi.org/10.1107/S0021889807067908)

35. L. J. Farrugia, *J. Appl. Cryst.* **45** (2012) 849 (https://doi.org/10.1107/S0021889812029111)

36. W. Geary, *Coord. Chem. Rev.* **7** (1971) 81 (https://doi.org/10.1016/S0010-8545(00)80009-0)

37. D. Lomjanský, C. Rajnák, J. Titis, J. Monco, L. Smolko, R. Boča, *Inorg. Chim. Acta* **483** (2018) 352 (https://doi.org/10.1016/j.ica.2018.08.029)

38. A. Tavman, *Spectrochim. Acta A* **63** (2006) 343 (https://doi.org/10.1016/j.saa.2005.05.020)

39. D. Kanamori, Y. Yamada, A. Onoda, T. A. Okamura, S. Adachi, H. Yamamoto, N. Ueyama, *Inorg. Chim. Acta* **358** (2005) 331 (https://doi.org/10.1016/j.ica.2004.09.014)

40. V. M. Leovac, L. S. Jovanović, V. S. Čečljević, L. J. Bjwlica, V. B. Arion, N. V. Gerbelu, *Polyhedron* **13** (1994) 3005 (https://doi.org/10.1016/S0277-5387(00)83421-X)

41. N. Sundaraganesan, C. Meganathan, B. Anand, C. Lapouge, *Spectrochim. Acta A* **66** (2007) 773 (https://doi.org/10.1016/j.saa.2006.04.025)

42. D. Mahadevan, S. Periandy, M. Karabacak, S. Ramalingam, *Spectrochim. Acta A* **82** (2011) 481 (https://doi.org/10.1016/j.saa.2011.07.082)

43. P. E. Kazin, M. A. Pogosova, L. A. Trusov, I. V. Kolesnik, O. V. Magdysyuk, R. E. Dinnebier, *J. Solid State Chem.* **237** (2016) 349 (https://doi.org/10.1016/j.jssc.2016.03.004)
44. K. Nakamoto, *Infrared and Raman Spectra of Inorganic and Coordination Compounds, Part B*, 5th ed., John Wiley & Sons, New York, USA, 1997
45. A. *Tavman*, A. Z. Elmal, D. Gürbüz, M. Hacioglu, A. S. Birteksöz Tan, A. Cinarli, *Rev. Roum. Chim.* **68** (2023) 49 (https://doi.org/10.33224/rrch.2023.68.1-2.05).